

Fabrication of sub-micron protein-chitosan electrostatic complexes for encapsulation and pH-Modulated delivery of model hydrophilic active compounds

Kurukji, Daniel; Norton, Ian; Spyropoulos, Fotios

DOI:

[10.1016/j.foodhyd.2015.02.021](https://doi.org/10.1016/j.foodhyd.2015.02.021)

License:

Creative Commons: Attribution (CC BY)

Document Version

Publisher's PDF, also known as Version of record

Citation for published version (Harvard):

Kurukji, D, Norton, I & Spyropoulos, F 2016, 'Fabrication of sub-micron protein-chitosan electrostatic complexes for encapsulation and pH-Modulated delivery of model hydrophilic active compounds', *Food Hydrocolloids*, vol. 53, pp. 249-260. <https://doi.org/10.1016/j.foodhyd.2015.02.021>

[Link to publication on Research at Birmingham portal](#)

Publisher Rights Statement:

Eligibility for repository : checked 19/08/2015

General rights

Unless a licence is specified above, all rights (including copyright and moral rights) in this document are retained by the authors and/or the copyright holders. The express permission of the copyright holder must be obtained for any use of this material other than for purposes permitted by law.

- Users may freely distribute the URL that is used to identify this publication.
- Users may download and/or print one copy of the publication from the University of Birmingham research portal for the purpose of private study or non-commercial research.
- User may use extracts from the document in line with the concept of 'fair dealing' under the Copyright, Designs and Patents Act 1988 (?)
- Users may not further distribute the material nor use it for the purposes of commercial gain.

Where a licence is displayed above, please note the terms and conditions of the licence govern your use of this document.

When citing, please reference the published version.

Take down policy

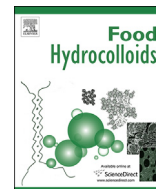
While the University of Birmingham exercises care and attention in making items available there are rare occasions when an item has been uploaded in error or has been deemed to be commercially or otherwise sensitive.

If you believe that this is the case for this document, please contact UBIRA@lists.bham.ac.uk providing details and we will remove access to the work immediately and investigate.



Contents lists available at ScienceDirect

Food Hydrocolloids

journal homepage: www.elsevier.com/locate/foodhyd

Fabrication of sub-micron protein-chitosan electrostatic complexes for encapsulation and pH-Modulated delivery of model hydrophilic active compounds

Daniel Kurukji*, Ian Norton, Fotis Spyropoulos

School of Chemical Engineering, University of Birmingham, UK

ARTICLE INFO

Article history:

Received 9 October 2014

Received in revised form

10 February 2015

Accepted 17 February 2015

Available online xxx

Keywords:

Chitosan

Caseinate

BSA

Complexes

Coacervates

Ultrasound

Sonication

Sub-micron

Encapsulation

pH

Actives

Colloidal

Colloids

Controlled

Targeted

Delivery

Release

Agrochemicals

Pharmaceuticals

Food

Modulated

Triggered

ABSTRACT

Electrostatic sub-micron complexes of a protein (sodium caseinate (NaCAS) or bovine serum albumin (BSA)) and a polysaccharide (chitosan) were fabricated by associative phase separation and investigated for use in encapsulation and pH-triggered delivery applications. Various factors have been studied with respect to the extent of complexing and the size and morphology of the complexes produced, including protein type and the biopolymer mixing ratio. The effect of applying ultrasound has been considered with a view to comminuting precipitates produced under low shear to the colloidal scale to form coacervates. A simple model is suggested to explain how the biopolymer mixing ratio influences the ability for application of ultrasound to convert macroscopically phase-separated complex precipitates into coacervates. Different factors, both from a formulation and processing viewpoint, were studied with respect to encapsulation efficiency (EE) of model hydrophilic actives: fluorescein, rhodamine B, and riboflavin. Release of fluorescein and rhodamine B was measured as function of pH in order to investigate the pH-responsive molecular release capability of the fabricated structures. It is envisaged this work will add to the current tool-box of pH-responsive molecular delivery approaches, including those in the areas of foods, pharmaceuticals, and agrochemicals.

© 2015 The Authors. Published by Elsevier Ltd. This is an open access article under the CC BY license (<http://creativecommons.org/licenses/by/4.0/>).

1. Introduction

Proteins and polysaccharides are polymers ubiquitous in nature. Research into how they interact, in addition to their behaviours at surfaces and interfaces, has long been undertaken (Dickinson, 2006; Rodríguez Patino & Pilosof, 2011). Due to the diverse range of chemical functionalities available, biopolymers can be assembled

into supramolecular structures held together by interbiopolymer forces. Controlling the type and relative magnitude of these forces enables production of a wide range of material properties, and potentially, the prospect of physically compartmentalising compounds (i.e. functional ingredient encapsulation), a feature often considered desirable for functional food, pharmaceutical, and agrochemical formulation design (Chen, Remondetto, & Subirade, 2006; Hack et al. 2012; Madene, Jacquot, Scher, & Desobry, 2006).

In a binary biopolymer system containing a protein and polysaccharide, the net interaction between the biopolymers can be

* Corresponding author. Tel.: +44 (0) 7414 861610.

E-mail address: djk080@bham.ac.uk (D. Kurukji).

associative (complexing) or segregative (repulsive), depending on the precise structures of the biopolymers present and the prevailing conditions, i.e. pH, ionic strength, and mixing conditions (Dickinson, 1998; Syrbe, Bauer, & Klostermeyer, 1998; Tolstoguzov, 1991). Whilst it is recognised that such interactions impart many of the functional properties of foods, further research is required to develop uses in encapsulation and targeted delivery of active ingredients. “Active ingredients” in the broadest sense include crop protection products, pharmaceuticals, and nutrients.

One way to encapsulate functional molecules in protein-polysaccharide complexes involves ‘bottom-up’ self-assembly of the constituent biopolymers. If an active is included during or after complex assembly it can become entrapped—physically or chemically—within the biopolymer matrix. When the biopolymers contain ionising groups, such as those found on polypeptide side chains and polysaccharides, an electrostatic force predominates that holds the newly-formed complex together; complexes produced in this way have potential application as pH-responsive materials that can assemble and dissociate under pH control. From a green and sustainable design viewpoint, biopolymers often have good biocompatibility and toxicity profiles, in addition to being derived from under-utilised resources; transition to use of sustainable materials may reduce the dependency on petrochemical-derived synthetic materials often used in non-food applications (Doi, Clark, Macquarrie, & Milkowski, 2002).

In this study we focus on using chitosan and protein as biopolymer building blocks for complex formation. Chitosan, a polysaccharide derived from crustaceans (e.g. crab shells) has received attention for use in pharmaceutical/biomedical applications (Bugamelli, Raggi, Orienti, & Zecchi, 1998; Qin, Zhu, Chen, & Zhong, 2007), and increasingly, for food nutraceutical encapsulation (Chen et al. 2006), in addition to emulsion interfacial structure development (Ogawa, Decker, & McClements, 2003, 2004); more broadly, chitosan is regarded as a sustainable material with applications ranging from catalysis to water purification (Macquarrie & Hardy, 2005). The versatility and uniqueness of chitosan originates in its chemical structure: the preponderance of amine groups on the polysaccharide backbone makes it the only naturally-derived cationic biopolymer. Protonation of these amine groups enables chitosan to be solubilised and easily manipulated in mildly acidic conditions (e.g. dilute acetic acid). Chitosan's chemical structure is also responsible for its mucoadhesive property (Sogias, Williams, & Khutoryanskiy, 2008; Sogias, Williams, & Khutoryanskiy, 2012), which has been considered in various drug delivery contexts.

Although chitosan has not been marketed in any drug products, it has received attention for possible applications in drug delivery, muco-adhesive dosage forms, rapid release forms, improved peptide delivery, colonic drug delivery systems and for gene delivery (Baldrick, 2010). Human exposure to chitosan has occurred, though not in pharmaceutical application, through dietary supplements designed for treating obesity and hypercholesterolaemia. For foods, chitosan has been designated as: Generally Recognised as Safe (GRAS) in the USA; it is listed as a food additive in Japan, Finland, and Italy (Baldrick, 2010).

In comparison to polysaccharides it is well known that proteins differ both in structure and function. Caseins and related caseinates, which are naturally occurring milk proteins, are often used in food products as emulsifying agents for stabilisation of emulsions and foams; this contrasts with the majority of polysaccharides, including chitosan, which have minimal surface activity, and as such, are mainly used for rheology-control and/or water-holding (Dickinson, 2009). Sodium caseinate (NaCAS), which is typically produced from acid casein, is principally comprised of four water-soluble caseins (α_{s1} , α_{s2} , β , and κ) assembled together. Whilst a

significant body of research has been generated to understand how NaCAS adsorbs at surfaces and interfaces, focus has recently shifted to its use as a biocompatible, non-toxic nano-carrier for encapsulation of vitamins and nutraceuticals (Semo, Kesselman, Danino, & Livney, 2007). Other research articles have demonstrated that chitosan forms complexes with a wide range of both globular and ‘disordered’ proteins (Anal, Tobiassen, Flanagan, & Singh, 2008; Huang, Sun, Xiao, & Yang, 2012; Lee & Hong, 2009; Yu, Hu, Pan, Yao, & Jiang, 2006). One of earliest studies investigated the precipitation of casein directly from milk for potential use in cheese making (Ausar et al. 2001). However, additional studies are required to develop complexes that enable pH-modulated delivery of functional molecules. This approach has a number of useful applications across foods, pharmaceuticals and agrochemicals.

To this end, the first part of this work investigates the complexation of chitosan and two proteins – sodium caseinate (NaCAS) or bovine serum albumin (BSA) – to evaluate how protein type influences the extent of complexing and the type of complexes produced (i.e. soluble versus insoluble complexes (precipitates or coacervates?)). BSA and NaCAS differ markedly in structure, with NaCAS being amorphous (Kontogiorgos, Ritzoulis, Biliaderis, & Kasapis, 2006) and BSA being globular crystalline (Ikeda & Nishinari, 2001). We consider how these differences in structure affect the extent of complexing and type of complexes produced under comparable processing and solution conditions.

Recently, ultrasound has been promoted as a possible route for modifying the functional properties of biopolymers (O'Sullivan, Arellano, Pichot, & Norton, 2014). The effect that ultrasound has on a molecule/polymer is related to the applied cavitation (rapid formation and collapse of bubbles) generated by localized changes in pressure and temperature. Most work in this area has been directed towards investigating ultrasound processing of single a biopolymer in solution or suspension. In particular, O'Sullivan et al. have noted that the effect of ultrasound on the functional properties of various food proteins leads to contradictory understanding, especially with regard to whether it can reduce protein molecular weight (O'Sullivan et al., 2014). It has been reported that ultrasound can reduce the molecular weight of chitosan, whilst not affecting the degree of acetylation (Wu, Zivanovic, Hayes, & Weiss, 2008). The effect of applying ultrasound to preformed mixed protein-polysaccharide complexes has received much less, if any, attention, although the effect of applying it to a kappa-carrageenan (solution) prior to complexing with a protein has previously been studied (Hosseini et al. 2013). In this work, we investigate the impact of applying ultrasound to pre-formed insoluble macroscopically phase separated protein-chitosan complexes initially formed under low shear.

Soft particles at the colloidal scale (e.g. coacervates) are potentially more useful than larger complexes/precipitates for encapsulation/controlled release application, as they are more stable to sedimentation, as well as possessing a greater surface area for molecular delivery of the encapsulated active. Furthermore, biopolymer complex colloidal suspensions (coacervates) often have similar rheological properties to oil-in-water emulsions which mean they could potentially be included within such products for controlled active or nutrient delivery.

The second part of the work goes on to demonstrate the potential for, and investigate some of the parameters that affect, the ability for various model active compounds to be encapsulated during mixed protein-chitosan complex formation. Typical formulation and processing parameters are considered in order to probe parameters that could potentially impact on encapsulation efficiency (EE). pH changes are then considered with respect to a triggering mechanism for release of the encapsulated active. It is envisaged that the information generated in this work will be

useful for the functional food design tool-kit, in addition to contributing to the design of new formulations across other sectors (e.g. agrochemicals, pharmaceuticals, etc) which could benefit from the pH-modulated delivery functionality. Typical examples of pH-modulated delivery include protection and/or triggered release of the active payload at different sites within the human gastrointestinal tract (pharmaceuticals, foods) or to different parts of the ecosystem (agrochemicals).

2. Experimental

2.1. Materials

BSA (lyophilised powder, $\geq 96\%$ purity); NaCAS (CAS: 9005-46-3); acetic acid ($\geq 99.7\%$ purity); low molecular chitosan (MW: 50–190 kDa) with de-acetylation degree of $>75\%$; fluorescein sodium salt (FSS) (CAS: 518-47-8); rhodamine B (Rhod B (CAS: 81-88-9)); and riboflavin (CAS: 83-88-5) were obtained from Sigma Aldrich, UK. All materials were used directly from the manufacturer without further purification. All water used in this study was passed through a double-distillation column equipped with a de-ionisation unit.

2.2. Methods

2.2.1. Protein-chitosan complex preparation without encapsulated actives

A stock solution of 1% protein (either NaCAS or BSA) was prepared under stirring by dissolving the desired amount of protein into 30 mM sodium acetate buffer at pH 5; this solution was left to stir for ca. 2 h. At pH 5 NaCAS existed partly as dewatered particles (this will be explained more fully in the results and discussion section). A BSA solution at the same concentration and pH was transparent indicating higher protein solubility. A separate stock solution (1% chitosan, 2% acetic acid, 97% water) was prepared under stirring until complete hydration of the polysaccharide. The pH of this solution was ca. 3. For a set of experiments a proportion of this stock chitosan solution was adjusted under vigorous stirring to pH 5 with 10% sodium hydroxide (NaOH).

All protein-chitosan mixtures were defined by total biopolymer concentration (TBC), mass proportion of total biopolymer present that is protein (M_{protein}), and mass proportion of total biopolymer present that is chitosan (M_{chit}). TBC in wt%, M_{chit} , and M_{protein} in the suspensions were defined by equations [1], [2], and [3]:

$$\text{TBC} = \frac{m_{\text{chit}} C_{\text{chit}} + m_{\text{protein}} C_{\text{protein}}}{T_s} \quad (1)$$

$$M_{\text{chit}} = \frac{m_{\text{chit}} C_{\text{chit}}}{T_s} \quad (2)$$

$$M_{\text{protein}} = 1 - M_{\text{chit}} \quad (3)$$

where m_{chit} is the mass in g of chit stock solution of concentration C_{chit} (wt%), m_{protein} is the mass (g) of protein solution of concentration C_{protein} (wt%), and T_s is the total mass of suspension. T_s of suspension was fixed at 50 g. As an example, to make a TBC of 2% at a $M_{\text{chit}} = 0.25$ required mixing 37.5 g of 2% protein solution at pH 5 (as in preparation of stock solution described above) with 12.5 g of 2% chitosan solution at pH 5 (as in stock solution preparation as described above). Similarly, a suspension containing the same ratio of biopolymers but at 1% TBC was produced in the same manner but starting with 1% stock solutions of both protein and chitosan. NaCAS-chitosan insoluble complexes were formed spontaneously

by addition of the correct amount of chitosan solution at pH 5 to NaCAS stock solution (pH 5) under low shear (i.e. on a magnetic stirrer) to make the desired TBC, M_{chit} , and M_{protein} . These suspensions were subjected to ultrasonic processing (Viber Cell 750, Sonics, USA) using a 12 mm diameter probe for 2 min (20 kHz, 95% amplitude).

Insoluble BSA-chitosan complexes were formed by heating mixtures under low shear containing the desired TBC, M_{chit} , and M_{protein} to 90 °C and then cooling in an ice bath to ambient temperature. After cooling, these suspensions were subjected ultrasonic processing (Viber Cell 750, Sonics, USA) using a 12 mm diameter probe for 2 min (20 kHz, 95% amplitude), in the same way as for the NaCAS-chitosan complexes described previously.

2.2.2. Particle size analysis

z-average particle diameter (also known as the hydrodynamic diameter) of the resulting complexes was obtained by dynamic light scattering (DLS) using the Zetasizer Nano Series (Nano ZS) (Malvern, UK). Two drops of concentrated protein-chitosan complex suspension were diluted into 25 g 30 mM sodium acetate buffer at original suspension pH (pH 5); this was immediately transferred to a polystyrene cuvette and measured.

2.2.3. Zeta potential

Zeta-potential analyses were performed on the Zetasizer Nano Series (Nano ZS) equipped with MPT-2 multipurpose titrator (Malvern, UK). For zeta-potential measurements of complexes made at varying M_{chit} , the given suspensions were diluted in the same way as for size analyses and added to a specialized zeta cell (Malvern, UK). Zeta potentials were reported for triplicate readings of three freshly prepared samples.

2.2.4. Turbidity titration for BSA-chitosan complexation

BSA-chitosan soluble complex formation was monitored using a turbidity titration. 45 g of 0.5% BSA solution was titrated with 0.5% chitosan solution incrementally. This was performed at pH 3, 5, and 6. 1 mL aliquots of the solution were taken after each addition of chitosan and the solution absorbance was immediately measured using ultraviolet–visible (UV-VIS) spectrometer (Libra S12, Biochrom, UK) at 420 nm. Selected solutions were stored under quiescent conditions after being partially titrated at ambient temperature, and their absorbance changes monitored over time; this gave an indication of BSA-chitosan complex stability.

2.2.5. Microscopy

Selected suspensions (in particular those containing large protein-chitosan precipitates) were analysed by optical microscopy (Brunel Microscopes Ltd SP300F, UK) equipped with a camera (Canon EOS 1000D, Japan). A drop of suspension was placed on a glass slide with a cover slip and then analysed. This suspension after sonication was visualised using a Phillips XL30 FEG Cryo Scanning Electron Microscope equipped with a Gatan low temperature unit. A single drop of suspension was placed on an analysis slide and dipped into nitrogen at -198 °C. This slide was then inserted directly into a preparation chamber at -180 °C where it was fractured and subsequently etched for 5 min at -90 °C to minimize ice formation. The surface was coated in gold and then imaged in the SEM at -130 °C.

2.2.6. Encapsulation of model actives

Encapsulation of model actives—fluorescein (FSS), rhodamine B (Rhod B), and riboflavin (Ribo)—was investigated. Chemical structures of these actives are provided in Table 1.

The encapsulation of FSS was studied at varying TBC (0.25, 0.5, 1, and 2%) and pH (5 and 7) as well as varying M_{chit} and M_{protein} .

Table 1
Model hydrophilic actives used.

Active	Chemical structure
Fluorescein	
Rhodamine B	
Riboflavin	

Encapsulation of Rhod B and Ribo were performed at a fixed TBC and at pH 5 to serve as a comparison with FSS. To perform the encapsulation, a solution of active was separately prepared in a 30 mM sodium acetate solution (adjusted to pH 5 or 7). The concentration of this active solution was fixed across all experiments and chosen to enable accurate analysis by UV-VIS without additional dilution steps (i.e. this concentration at the upper end of the concentration versus absorbance linear range). The stock concentrations used for each model active were as follows: FSS: 0.2 mg g⁻¹, Rhod B: 0.007 mg g⁻¹, and Ribo: 0.05 mg g⁻¹. Solutions of protein and chitosan biopolymers at the desired TBC were separately prepared as described previously and adjusted to the desired pH (pH 5 or 7) using 10 wt% HCl or NaOH. 5.5 g of the stock active solution was added to the protein solution before complexation. The desired amount of chitosan solution was then added drop-wise to the protein plus active solution under stirring. This suspension was subjected to ultrasonic processing (Viber Cell 750, Sonics, USA) under the same conditions as described previously.

Encapsulation efficiency (EE) in % was determined for the complexes by transferring 1.5 mL of suspension before and after sonication to separate Eppendorf tubes and centrifuging (Sigma 3k30, SciQuip, UK) for 60 min at 15,000 rpm (20 °C); this centrifugation time was determined in preliminary experiments as sufficient to separate the complexes as an insoluble pellet at the bottom of the Eppendorf tube. The supernatant was analysed by UV-VIS (Libra S12, Biochrom, UK) at the following wavelengths for each active: FSS = 460 nm, Rhod B = 550 nm, and Ribo = 460 nm. Using Beer's law the concentration of active in the supernatant was calculated over its linear range by calibration. EE was then calculated using equation [4]:

$$EE = \left(1 - \frac{C_{sup}}{C_{max}}\right) 100 \quad (4)$$

where C_{sup} is the concentration of active in the supernatant after centrifugation and C_{max} is the total concentration of active introduced into the system.

2.2.7. Release studies

Release of FSS and Rhod B from the complexes was monitored as a function of pH with a glass pH probe and meter (SevenEasy, Mettler Toledo, Switzerland) at a fixed TBC (1%) and $M_{chit} = 0.25$. In a release experiment, 55.5 g of suspension containing the active at

pH 5 was stirred in a 50 mL beaker on a magnetic plate. Small (50–1000 µL) 10% NaOH aliquots were added in pH intervals up from pH 5 to ca. pH 11. Only 2–3 mL of 10% NaOH in total was required for this adjustment. When each pH interval had been reached, a 1.5 mL aliquot was withdrawn from the suspension and transferred to an Eppendorf tube. These withdrawn samples were centrifuged (Sigma 3k30, SciQuip, UK) at 15,000 for 60 min and the FSS concentration in the supernatant was determined, as per the EE determination.

Due to its acid-base chemistry it was not possible to quantify FSS concentration at low pH (i.e. <pH 5); therefore, Rhod B was preferentially used to monitor entrapment/release at pH < 5. For Rhod B, the complex suspension was first titrated down to pH 2 using 50–1000 µL aliquots of 10% HCl and then back up to pH ca. 11 with 50–1000 µL aliquots of 10% NaOH. 1.5 mL samples were taken in intervals as described previously. FSS has an isosbestic point at 460 nm, which enabled its concentration to be obtained independent of the pH change. Rhodamine B and riboflavin did not exhibit a pH dependency on absorbance at the wavelengths employed for their analysis in the UV-VIS spectrophotometer.

Release profiles are presented as %active released from the complexes; the amount of active initially entrapped by the complexes ($C_T - C_{i,sup}$) at pH 5 was calculated by subtracting the initial concentration of active in the supernatant ($C_{i,sup}$) after entrapment at pH 5 from the total active concentration in the system (C_T). % active released was then calculated by measuring the additional increase in active concentration in the supernatant as a function of pH ($C_{f,sup} - C_{i,sup}$) divided by the initial concentration of active entrapped ($C_T - C_{i,sup}$):

$$\% \text{ release} = \frac{C_{f,sup} - C_{i,sup}}{C_T - C_{i,sup}} 100 \quad (5)$$

A schematic is presented in Fig. 1 to outline the general experimental approach presented in this work.

3. Results and discussion

3.1. Protein-chitosan complexing under low shear – influence of protein type

Preliminary work focussed on comparing the complexing of chitosan with two different proteins under low shear (i.e. magnetic stirring). NaCAS and BSA were chosen as they adopt different conformations in aqueous solution, with the former being an unfolded protein and the latter a globular protein. Complexing of chitosan with each protein was performed at pH 5, a condition favouring associative phase separation (i.e. where individual biopolymer charges were opposite). Few studies have investigated complexation close to the IEP of the protein, and, at least for NaCAS, this meant an initial suspension containing a significant amount of insoluble protein particles.

The first part of the work considered the complexation of NaCAS with chitosan at pH 5 under low shear magnetic stirring. At pH 5 NaCAS had a modest negative charge causing self-association of the individual NaCAS molecules resulting in partial NaCAS phase separation. This was a consequence of the NaCAS solution pH being close to the NaCAS' isoelectric point (IEP) (IEP of NaCAS ~ 4.6 (Girard & Schaffer-Lequart, 2008)). Mixing NaCAS and chitosan solutions under low shear within the region (TBC 0.25–2%) resulted in associative phase separation caused by charge neutralisation interactions occurring between chitosan and NaCAS. Visualisation by light microscopy of these complexes revealed macro-sized, irregular biopolymer complexes (see Fig. 2), and this particle morphology was typical of complexes formed across the range of

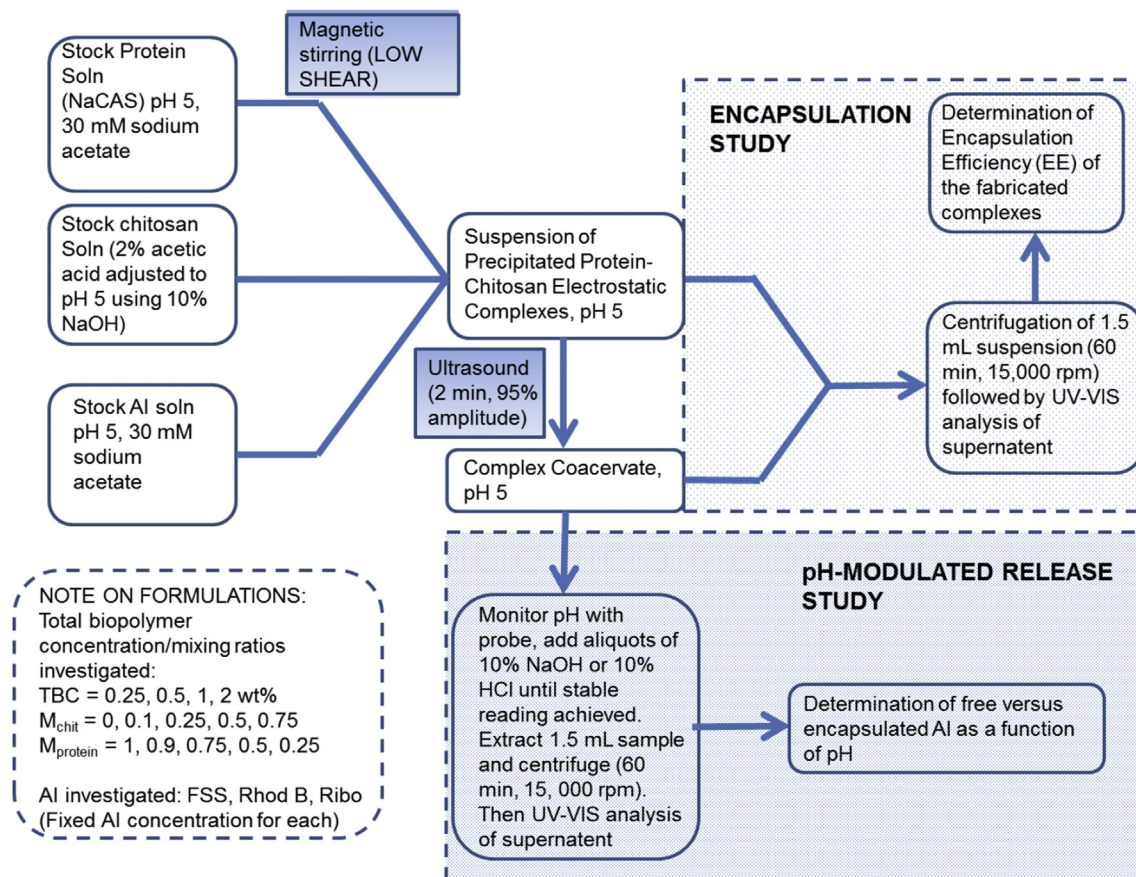


Fig. 1. Schematic of experimental approach.

NaCAS-chitosan biopolymer mixing ratios (M_{chit} = 0.1–0.75) and TBCs (0.1–2%) investigated in this work. This demonstrated that low shear mixing of NaCAS and chitosan solutions resulted in macroscopic phase separation to produce inter-biopolymer precipitates. Such precipitates can be distinguished from coacervates, as the latter are generally characterised as insoluble complexes (a biopolymer rich phase) suspended as liquid droplets throughout a

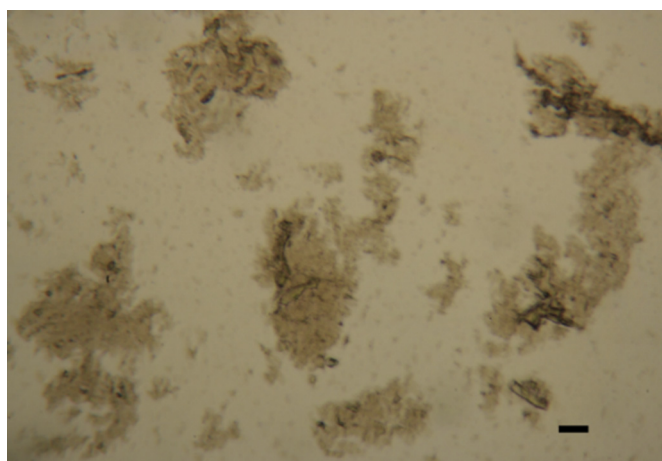


Fig. 2. Representative light micrograph showing morphology of NaCAS-chitosan complex precipitates formed under low shear. M_{chit} = 0.25. TBC = 1%. Scale bar = 100 μm . Comparable complex morphology was observed across the range of biopolymer mixing ratios and total biopolymer concentrations investigated: TBC = 0.25–2% and M_{chit} = 0.1–0.75.

biopolymer depleted solvent continuous phase (Harnsilawat, Pongsawatmanit, & McClements, 2006). However, the insoluble complexes shown in Fig. 2 did not exhibit this defining characteristic and are therefore classified as precipitates.

Upon changing the protein type from NaCAS to BSA and mixing the biopolymer solutions under equivalent solution (ionic strength, TBC, pH) and processing conditions (low shear magnetic stirring), the large-scale associative phase separation to produce precipitates observed in the NaCAS-chitosan system was not apparent. Instead, a single phase system comprising colloidal BSA-chitosan complexes was observed. Further work also revealed that the complexes formed between chitosan and BSA were transient and their presence strongly influenced by the BSA-to-chitosan mixing ratio. A turbidity titration was employed to monitor BSA-chitosan particle formation at pH 3, 5, and 6 (Fig. 3a); this approach is often used to study particle formation during biopolymer complexing, as solution turbidity is related to particle size and concentration (Weinbreck, de Vries, Schrooyen, & de Kruijff, 2003).

Fig. 3a shows solution absorbance as a function of the biopolymer mixing ratio (expressed as a function of chitosan concentration) at different pHs. At pH 3 where the net charge on both BSA and chitosan was positive (the pH was below the pKa of chitosan and also below the IEP of BSA), the electrostatic driving force for biopolymer complexation was low, and the measured absorbance remained constant at baseline level across all the mass ratios of BSA-to-chitosan measured. Under this condition it was probable that the biopolymers' preferred thermodynamic state was cosolubility: this was likely a consequence of each biopolymer charge becoming positive, which reduced the electrostatic driving force for association into biopolymer complexes.

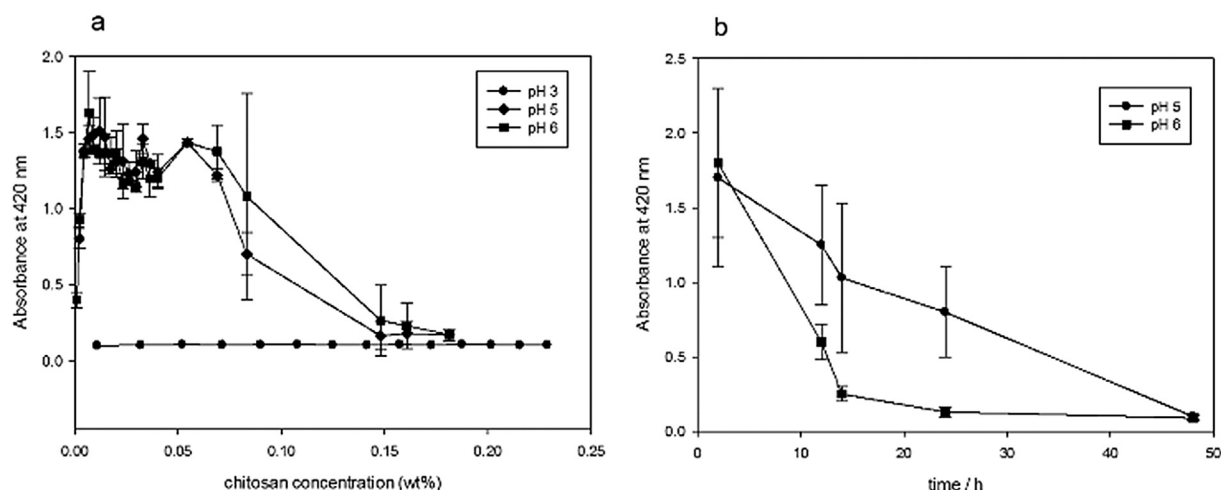


Fig. 3. (a) turbidity titrations of BSA with chitosan at pH 3, 5, and 6. (b) absorbance–time profiles of suspensions for titrations stopped at a chitosan concentration = 0.05% and periodically measured over time.

Upon increasing the pH to 5 or 6 the charge on each biopolymer became opposite, with chitosan possessing a net positive charge and BSA a negative charge. Under this condition, as chitosan is titrated into the BSA solution, particles form by biopolymer association and the solution turbidity increases. However, a key difference compared to the NaCAS–chitosan system was that only a single phase system could be produced, which visually appeared colloidal in nature (as opposed to demonstrating the large scale phase separation observed for the NaCAS–chitosan system). This suggested that the BSA–chitosan complexes formed had a higher solubility than the NaCAS–chitosan particles described previously. Beyond the absorbance maximum observed (in the region 0.01–0.05% chitosan), the turbidity then began to fall to baseline level with further addition of chitosan (see Fig. 3a). This suggested that the BSA–chitosan soluble particles had dissociated with increasing chitosan concentration, leading to either co-soluble biopolymers or soluble particles significantly smaller than the wavelength of the impinging light.

The stability of the BSA–chitosan soluble complexes was then measured. To achieve this, the titration described previously was stopped at a BSA-to-chitosan concentration ratio in the absorbance maximum region (0.05% chitosan) (Fig. 3b). The resulting sample was subsequently placed under quiescent storage at ambient temperature and its absorbance monitored over time. It can be seen in Fig. 3b that the turbidity reduced over time upon storage of the soluble complexes. This suggested that under the conditions of particle formation employed in this work, the BSA–chitosan complexes produced were only kinetically stable for 24–48 h, with a tendency towards dissociation, i.e. the thermodynamically favoured state under was either co-solubility of the biopolymers or “rearrangement/break-up” into smaller particles. It should also be noted that large experimental error did not allow for differences in dissociation rates at pH 5 or 6 to be measured. The large error in these experiments is probably due to microscopic inhomogeneity in complex size and concentration distributed throughout the samples, which could lead to differences in light scattering. The process/mixing condition was reproduced as precisely and accurately as possible; however, it was only possible to capture the general trends as a function of pH. The BSA–chitosan complex suspensions did not exhibit sedimentation, suggesting that macroscopic phase separation was not the cause of the large error.

It has previously been stated that when the strength of the interaction between the individual biopolymers is comparatively

large, then insoluble complexes or coacervates form, whereas when the interaction is weaker there is a tendency for the biopolymers to be co-soluble or to form soluble complexes (Hong & McClements, 2007). From experiments presented in this paper it is clear that protein structure has a major effect on the nature of the complexes formed under comparable solution and processing conditions. It is known that when biopolymers come into contact under pH conditions favouring association they interact at junction zones (Tolstoguzov, 2003). In the case of BSA–chitosan it is clear that these junction zones were unstable, since the biopolymers dissociated over short timescales. In contrast, the large interaction between NaCAS and chitosan seemed to force macroscopic association into insoluble biopolymer precipitates. For NaCAS–chitosan this may have been driven to some extent by the fact the initial NaCAS solution was at least partly phase separated (NaCAS showed some phase separation at pH 5). Tolstoguzov has previously stated that globular proteins cannot easily form contacts (junction zones) with linear rod-like polysaccharides such as chitosan owing to topological limitations, which contrasts with proteins that are unfolded such as casein, where the association interactions are greater (Tolstoguzov, 2003). The results obtained in this work appear to support this idea.

3.2. Ultrasound treatment of protein–chitosan precipitates

3.2.1. Production of colloidal NaCAS–chitosan insoluble complexes

Applications often require particles that remain stable to sedimentation (i.e. are colloidal). The application of ultrasound on the NaCAS-only and NaCAS–chitosan precipitates was thus investigated as a route to reduce the particle size. Firstly, ultrasound was applied to a NaCAS-only suspension at pH 5 (the control). Without chitosan being present in the formulation, the average particle diameter did not reduce to the colloidal scale, and protein precipitates were observed even after sonication resulting from the self-association of NaCAS close to its IEP. This is unsurprising since dispersing protein particles (to a colloidal size) is a thermodynamically unfavourable process and extremely difficult to achieve even using typical high energy processing options such as high pressure homogenization or ultrasound treatment (Dickinson, 2012).

Applying ultrasound to the NaCAS–chitosan precipitates produced under low shear, demonstrated a noticeable change in bulk suspension characteristics during sonication, depending primarily

on the biopolymer mixing ratio (M_{chit}). When $M_{\text{chit}} \geq 0.25$ the resulting bulk suspensions were converted into colloidal suspensions visually akin to typical oil-in-water emulsions. Fig. 4a shows DLS analysis of these suspensions, with sub-micron z-average particles sizes observed for $M_{\text{chit}} \geq 0.25$. This suggested a coacervate was formed upon the application of ultrasound to a NaCAS-chitosan precipitate, as long as the biopolymer mixing ratio was above a critical amount.

In terms of understanding the mechanism of coacervate formation, it is useful to consider why application of ultrasound at $M_{\text{chit}} = 0.1$ did not produce a coacervate. At this biopolymer mixing ratio the system remained macroscopically phase-separated with sedimented, irregular precipitates observed at the bottom of the sample vial, comparable in morphology to those shown in Fig. 2. It should be noted that DLS is an inaccurate particle sizing tool for particles produced at this mixing ratio (DLS is used for colloids where Brownian motion dominates), although a particle size measurement is reported in Fig. 4a with the correspondingly large error to emphasize the difference. This was deemed viable for the purposes of this work, as the trend was more important than reporting of absolute average particle sizes.

This biopolymer mixing ratio dependence on whether sonication could convert the precipitate into a coacervate suggested that inter-complex forces had a major effect on the dispersive effect of ultrasound in this system. Complexing of chitosan with NaCAS at pH 5 caused charge neutralisation of oppositely charged chemical groups present on NaCAS. NaCAS was at least partially phase separated at pH 5 (prior to addition of chitosan) resulting from its self-association into particles close to its IEP. When chitosan physically interacts with NaCAS at pH 5 it introduced a cationic charge repulsion between them. This cationic charge was probably caused by excess amine groups that do not participate in protein binding, thus conferring a cationic charge to the complex at pH 5. As can be seen in Fig. 4b, a NaCAS-only suspension at pH 5 (without chitosan present) possessed a modest zeta potential of -20 mV. It has previously been observed across many systems that a zeta-potential of at least ± 30 mV is required to introduce enough electrostatic repulsion to limit particle association (Heurtault, Saulnier, Pech, Proust, & Benoit, 2003). Therefore, the magnitude of negative charge observed in this work for a protein only slightly above its IEP demonstrates why a high degree of association was observed. As described previously, even sonication could not effectively disperse these NaCAS particles.

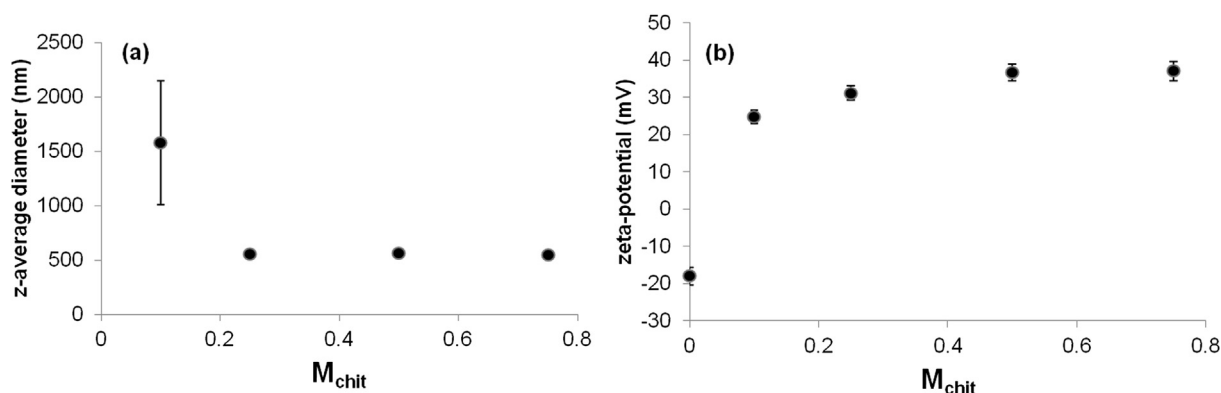


Fig. 4. (a) NaCAS-chitosan z-average complex diameter measured at pH 5 by DLS after ultrasound processing (2 min, 95% amplitude) at different NaCAS and chitosan mixing ratios. (b) zeta-potentials measured after ultrasound at different NaCAS and chitosan mixing ratios.

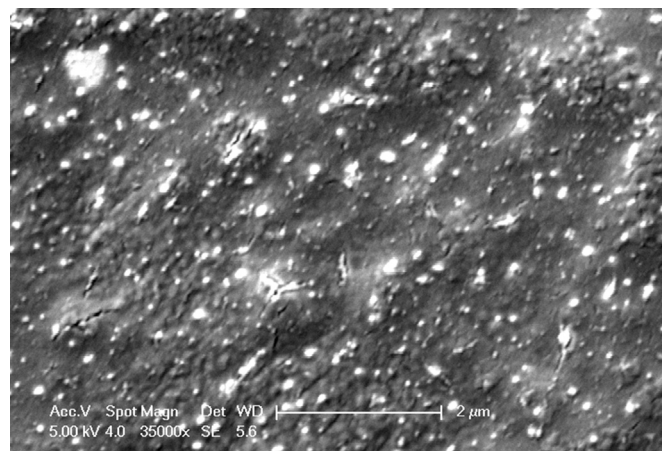


Fig. 5. Cryo-SEM micrograph of the NaCAS-chitosan complexes/coacervates formed after sonication of the preformed precipitates. $M_{\text{chit}} = 0.25$. TBC = 1%.

Addition of increasing chitosan to these NaCAS suspensions caused a charge reversal to limiting zeta potential of ca. 36 mV. Fig. 4b shows that charge neutralisation (zeta potential = 0) had occurred at a biopolymer mixing ratio between 0 and 10% chitosan ($M_{\text{chit}} = 0.1$); however, even at $M_{\text{chit}} = 0.1$, precipitates were observed. It is probably that although charge neutralization had been achieved, complete electrical coverage of the protein particles had not been obtained. A likely consequence of this was that the charge repulsion introduced between the complexes was insufficient to transfer the system from a precipitate to a coacervate (a colloid) upon sonication. As chitosan was increased above 25% of the total biopolymer concentration and in the limit of 75%, the zeta-potential approached a limiting value of ca. 36 mV. It was probable that complexes formed in this mixing region had sufficient chitosan present within them to provide effective charge repulsion between the complexes, resulting in generation of a colloidal suspension on application of ultrasound.

In order to compare the NaCAS-chitosan suspension after sonication (the coacervate) with the precipitates formed under low shear (see Fig. 2), cryo-SEM (Fig. 5) was employed. This technique is particularly versatile for this system as it enables structures to be visualised in their native environment as opposed to after dry-down where substantial structural changes are likely. The

micrograph in Fig. 5 shows the presence of sub-micron sized complexes which appear to have contrasting morphologies than complexes prepared under low shear (compare Fig. 2). In particular, the complexes appeared spherical or near spherical as opposed to irregular polymer clusters observed for the complexes prepared under low shear. It is also clear that the particle size is significantly smaller than for the precipitates shown in Fig. 2, and this supports the DLS measurements reported previously.

3.2.2. Production of sub-micron BSA-chitosan complexes

As discussed previously, BSA formed transient soluble complexes with chitosan under low shear mixing. However, in order to generate structures with an encapsulation/delivery functionality, a colloidal complex suspension (a coacervate) was preferred over a complex precipitate. To increase the number of junction zones available for chitosan and BSA to interact, thermal denaturation of BSA was investigated. Heating globular BSA above its denaturation temperature caused disruption of the intra-protein forces stabilising its higher order globular structure. The result of this process was formation of insoluble protein aggregates driven by the hydrophobic effect. In this work, BSA denaturation in the presence of chitosan was performed under equivalent solution (pH, ionic strength, TBCs) and processing conditions (low shear magnetic stirring) as for the NaCAS-chitosan system in order to provide a direct comparison.

Heating a BSA-only solution (anywhere in the region 0.25–2%) to 90 °C followed by cooling to ambient temperature resulted in protein phase separation, caused by BSA denaturation and a self-association mechanism to form BSA particles. BSA exhibited large scale phase separation and sedimented rapidly after heating, in a similar fashion to NaCAS at pH 5. In a similar manner to NaCAS it was observed that subjecting these BSA protein particles to sonication could not disperse them to the colloidal scale. However, performing the same denaturation process in the presence of chitosan resulted in precipitate formation. In a similar manner as the NaCAS-chitosan system, sonication could be employed to produce a BSA-chitosan complex coacervate containing sub-micron complexes. Again, the biopolymer mixing ratio strongly influenced whether a colloidal suspension (a coacervate) could be produced using ultrasound. Fig. 6a shows that a greater concentration of chitosan within the suspension was required to produce a BSA-chitosan complex coacervate than for the NaCAS system (see Fig. 4a for comparison). A BSA-chitosan coacervate could be formed

at $M_{\text{chit}} = 0.75$, whilst at the lower biopolymer mixing ratios the suspension contained large scale precipitates. The visual appearance in terms of its colloidal attributes of the BSA-chitosan suspension at $M_{\text{chit}} = 0.75$ was similar to the NaCAS-chitosan suspensions at $M_{\text{chit}} \geq 0.25$. These experiments suggested that as BSA was denatured it transferred from a globular to unfolded structure, which increased the number of junction zones available for its interaction with chitosan; this was also in-line with observations made previously concerning complexation of BSA with chitosan under ambient conditions.

The zeta-potential (Fig. 6b) data is also in-line with increased chitosan necessary for providing effective charge repulsion in the BSA-chitosan system: a zeta potential comparable to $M_{\text{chit}} = 0.25$ in the NaCAS system was achieved when $M_{\text{chit}} = 0.75$ in the BSA system. This again demonstrated the importance of charge repulsive effects necessary for producing a colloidal suspension during sonication. The fact that BSA required a higher concentration of chitosan than NaCAS to generate a colloidal suspension was probably due to a difference in net interactions occurring between the biopolymers, as influenced by protein molecular weight, amino acid sequence, and conformation.

3.3. Mechanistic considerations

To generalize some of the observations made previously, a proposed mechanism is provided schematically in Fig. 7 and outlined below.

1. As chitosan is added to the protein under low shear it becomes incorporated into the protein, interacting primarily by electrostatic interaction with oppositely charged groups on the protein, thus causing an increase in complex charge as observed via zeta potential analysis. The conformation of the protein impacts strongly on the extent of the interaction and hence the solubility of the complexes produced.
2. When protein-chitosan precipitates have been formed under low shear, subsequent application of ultrasound is strong enough to disrupt intermolecular forces between the protein particles but only under certain circumstances. When enough chitosan is present during sonication, the protein particles transfer from a bulk phase-separated precipitate to a colloidal suspension (a coacervate). This is driven by the level of charge repulsion introduced between the individual complexes.

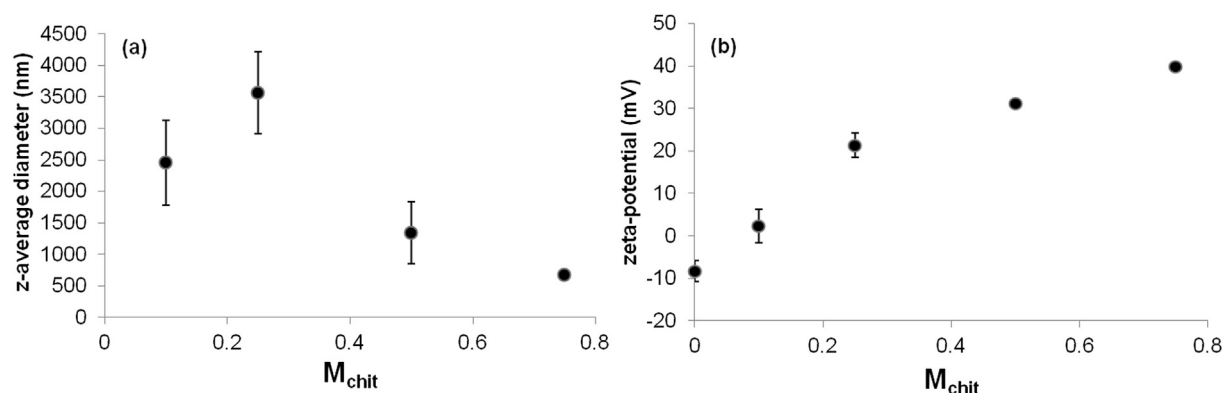


Fig. 6. BSA-chitosan z-average particle diameter measured at pH 5 by DLS after ultrasound processing of the denatured BSA-chitosan precipitates (2 min, 95% amplitude) at different mixing ratios of BSA and chitosan. (b) zeta-potentials measured after ultrasound at different mixing ratios of BSA and chitosan.

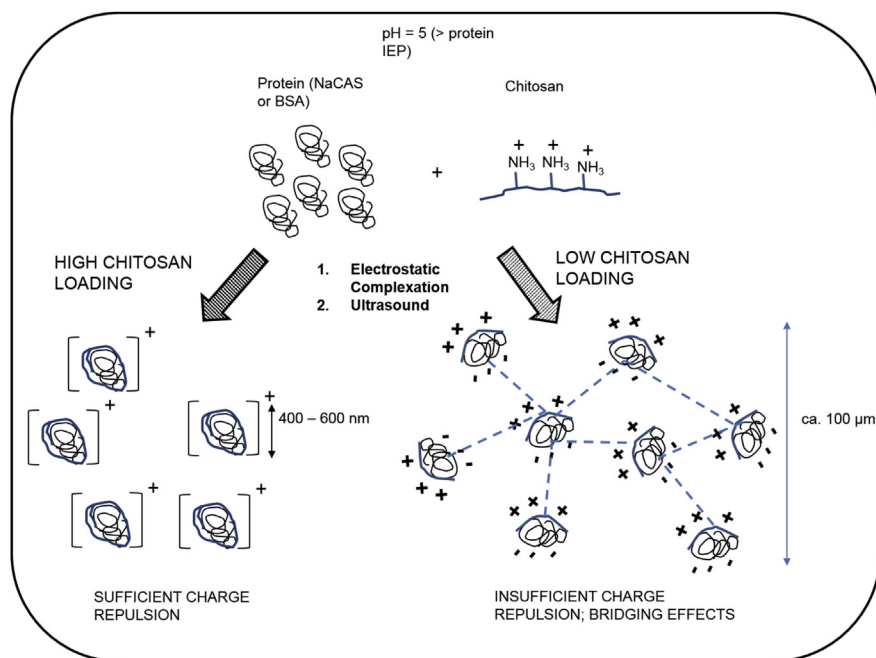


Fig. 7. Mechanistic schematic of sub-micron complex/coacervate formation.

3. A possible explanation for obtaining a precipitate (in the presence of chitosan but at low concentration) after sonication is that the anionic protein particles do not achieve full electrostatic coverage with chitosan, therefore leaving charged patches on surface of the protein particle; it is possible that this drives a bridging interaction between the individual complexes (see Fig. 7) resulting in their remaining in a precipitated state.

3.4. Encapsulation and release studies

3.4.1. Encapsulation efficiency (EE)

Complexes (both precipitates and coacervates) fabricated in this work were investigated for their use in encapsulation and pH controlled release of model hydrophilic active compounds. Initial work focussed on encapsulation of fluorescein sodium salt (FSS), with additional model compounds – rhodamine B (Rhod B) and riboflavin (Ribo) – being employed to further investigate the mechanisms involved. The main aim was to assess the interplay between pH, encapsulation, and release, as pH is a useful triggering mechanism relevant to food, pharmaceutical, and agrochemical formulation design.

The first experiments assessed the effect of different variables on encapsulation efficiency (EE). The ratio of chitosan-to-protein present (expressed as M_{chit} , where $M_{\text{protein}} = 1 - M_{\text{chit}}$), TBC, pH, and the effect of applying sonication were all studied.

Fig. 8 shows how M_{chit} and protein type influenced EE before and after sonication for a fixed TBC = 1%. The first point to make is that the presence of chitosan was not required for encapsulation of FSS in either system. FSS was encapsulated at pH 5 by both NaCAS- and BSA-only (see $M_{\text{chit}} = 0$). However, as discussed previously, the presence of chitosan was necessary for forming a colloidal suspension during sonication. Protein particles containing active formed without chitosan present were phase separated protein precipitates; this was true irrespective of whether this was driven by denaturation (as for BSA) or by precipitation (as for NaCAS). The resulting complexes, though possessing FSS encapsulation ability,

had a low surface area for active transfer, in addition to sedimenting rapidly resulting from the lack of colloidal stability. This made forming complexes (as opposed to using the protein-only) advantageous for molecular delivery.

The level of chitosan in the protein-chitosan complex suspensions also influenced the magnitude of EE. As shown in Fig. 8, at $M_{\text{chit}} = 0.75$ the amount of FSS that was encapsulated decreased significantly. When chitosan was added above and beyond that required for complete charge coverage of the protein, the zeta potential approached a constant value indicating that additional chitosan resided within the continuous phase (it did not form part of the complex). This is evident in Fig. 4b, for example. Therefore the reduction in EE could be attributed to competition between encapsulation of FSS into the complexes versus binding into freely soluble chitosan.

It was observed that sonication of the FSS-containing precipitates into coacervates did not reduce EE when chitosan was present in the formulation; however, it did reduce it slightly for both the protein-only cases. This suggested a different overall mechanism of active binding between the protein-only and protein-chitosan cases. It may be that the net interaction between FSS and protein particle matrix was weaker than for FSS and the protein-chitosan complex. However, additional experiments would be required to confirm this.

The fact that sonication did not dissociate FSS from the coacervate matrix pointed to a strong (i.e. electrostatic) force holding the active within its structure. This was further corroborated by Fig. 9 which shows how pH and TBC impact on FSS EE. At a pH favouring complexation (i.e. pH 5), the EE increased from ca. 65%–90% with increasing TBC. This TBC dependency on EE was to do with the total amount of biopolymer available for encapsulating the active: a higher biopolymer concentration meant more electrostatic binding sites available and therefore higher EE for a fixed active loading. However, at pH 7 the driving force for complex formation was reduced across all TBCs (i.e. the charge on chitosan was close to zero). Under this condition, the electrostatic driving force for assembling of the biopolymer complex with FSS was reduced,

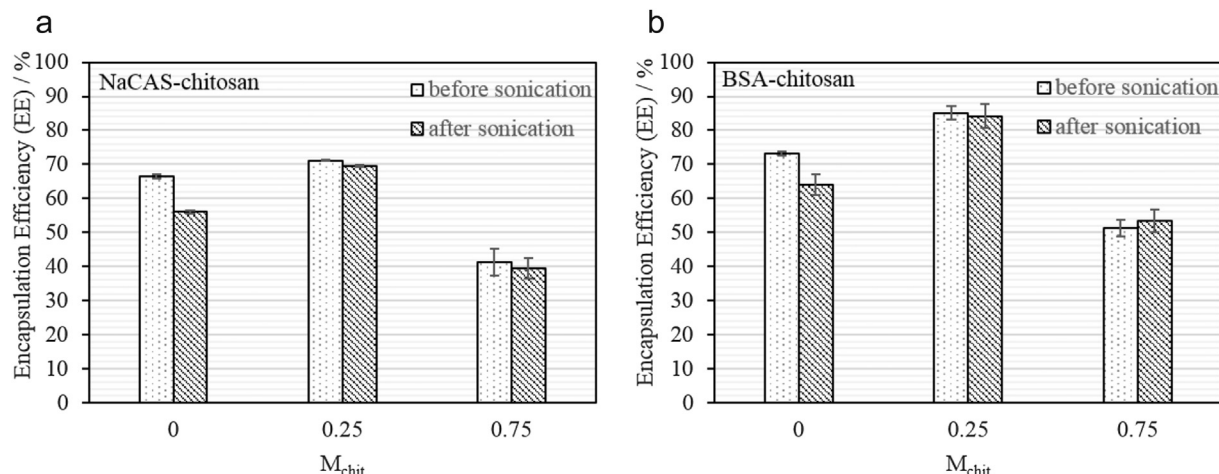


Fig. 8. Encapsulation efficiency (EE) of FSS at pH 5 within (a) NaCAS-chitosan and (b) BSA-chitosan complexes before sonication (dotted bars) and after sonication (striped bars) sonication. TBC was fixed at 1%.

although it was clear some favourable interactions occurred between the biopolymers and FSS. This could present itself as an interaction between FSS and self-associated chitosan at pH 7 (the pKa of chitosan ca. 6.5–7). The observed pH dependency on EE reiterates the importance of the FSS-biopolymer matrix electrostatic interaction discussed earlier, which strongly influenced the extent of FSS assembly with the biopolymer complex.

Two other actives (Rhod B and Ribo) were also tested for encapsulation at pH 5. Rhod B was chosen since it has a similar chemical structure, in terms of its aromatic acid group, to FSS (see Table 1), whereas Ribo, a water-soluble vitamin, contrasts with FSS and Rhod B in that it is a more basic molecule. Changing the active structure gave additional understanding of which functional molecules might be suited for encapsulation in the biopolymer complexes produced in this work.

Rhod B showed a similar EE to FSS (65%), whereas it was not possible to encapsulate any Ribo under equivalent processing conditions. As FSS and Rhod B are structurally similar (see Table 1), both containing an aromatic acid group, it is probable that this group participated via electrostatic interaction with the biopolymer

matrix. The idea that the active acid group-complex matrix interaction drives encapsulation was strengthened on observation that Ribo could not be encapsulated. Ribo does not possess the acid chemical group and therefore cannot participate in electrostatic intermolecular bonding. Thus, in general, chemical actives that contain an organic acid group or other anionic group at pH 5 are potential candidates for encapsulation in the protein-chitosan biopolymer complexes produced in this work. This encompasses actives across different sectors, including those found in pharmaceuticals, agrochemicals, and foods.

A final feature of the complexes worth mentioning is that FSS and Rhod B could also be loaded after complex formation, without impacting significantly on EE. This is an important process consideration, as it is often undesirable to subject actives to high energy processing operations such as high pressure homogenisation or sonication. Therefore, temperature or shear sensitive actives could potentially be encapsulated after structure formation, assuming they meet the other structural requirements. This increases the utility of the complexes as well as improving process flexibility.

3.4.2. Release of actives using a pH trigger

It is often desired to use an external trigger such as pH to stimulate release of active ingredients from colloidal carriers. Such materials are collectively known as 'smart' due to their ability to respond to external stimuli. Active carriers fabrication in this manner could be incorporated in various products to achieve a desired effect (e.g. to target release or to protect the active). To this end, the effect of pH on active release was examined. To achieve this, complexes containing FSS and Rhod B were fabricated at pH 5 and subjected to different pH environments. Fig. 10 shows %active (FSS and Rhod B) released from the NaCAS-chitosan coacervates as a function of pH.

As the pH was increased from 5 to above the pKa of chitosan (~6.5–7), the fraction of active released from the complexes increased from less than 5% to 70–80%; this release behaviour was consistent with a pH trigger release mechanism controlled by electrostatic assembly of the complexes and the active.

Rhod B release was examined at pH < 5 to determine if these complexes retained their payload under more acidic conditions. Fig. 10 confirmed that in the limit of pH 2, Rhod B release from the biopolymer coacervate was negligible; the coacervate remained intact at low pH with Rhod B residing within the sub-micron

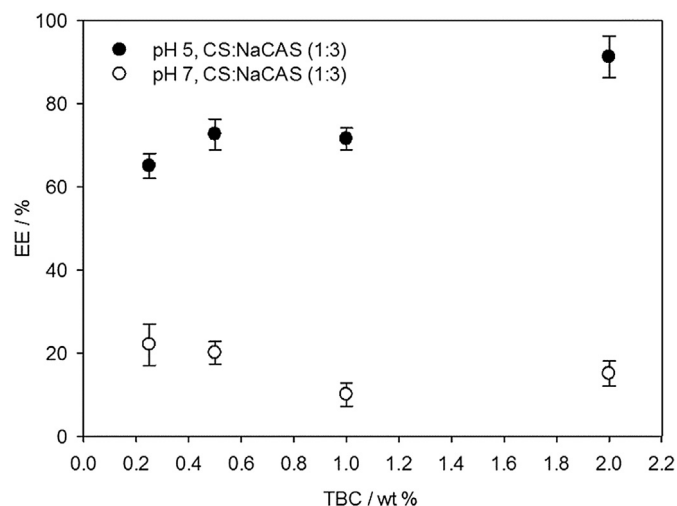


Fig. 9. EE as a function of total biopolymer concentration (TBC) at pH 5 (closed symbols) and pH 7 (open symbols). Biopolymer mixing ratio (as defined by M_{chit}) was fixed at 0.25.

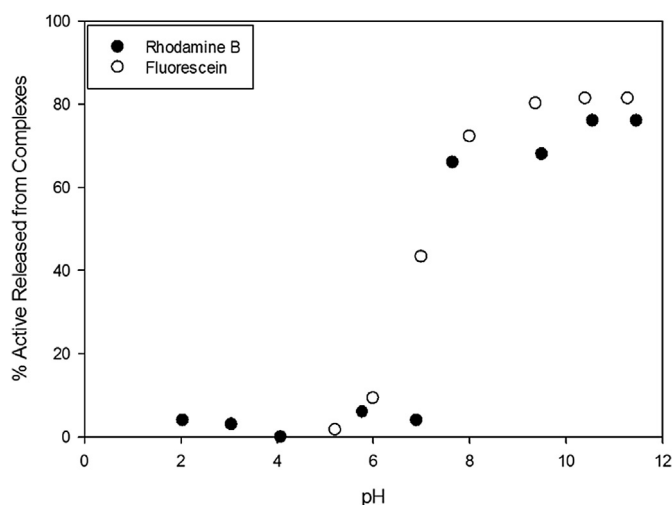


Fig. 10. Release of fluorescein (FSS) and Rhodamine B (Rhod B) from the fabricated coacervates as a function of pH. TBC = 1% and $M_{\text{chit}} = 0.25$.

complex. It is important to note that for both Rhod B and FSS the amount released did not reach 100%, meaning that some of active remained embedded within the dissociated biopolymers.

The release behaviour presented in Fig. 10 could prove useful in a number of applications, including targeted release within the human body. There is also potential for protecting acid-sensitive actives from degradation within the acidic environment of the human stomach, or for reducing stomach irritation. For food applications the structures would have to be formulated within acidic products (pH 5–6) since this would be necessary for maintaining complex stability. A key requirement of the active shown within this work is that it had to form a strong interaction (electrostatic) with the complex matrix. Since active release was influenced primarily by pH dependent degradation/dissociation of the complex and the electrostatic force holding the active within the particle structure means sites could potentially be targeted without “losing” active by diffusion to non-targeted sites. Overall, this has significant potential for the targeted release “tool-box”.

4. Summary and conclusions

This work demonstrates the use of protein-chitosan complexes for encapsulation and delivery of active compounds. The design rules for colloidal suspension fabrication have been discussed accounting for some of the key processing and formulation variables. Factors influencing encapsulation of model actives have been investigated, providing new insights for how these complexes could be used for pH-modulated molecular delivery. It should be noted that the functional molecules employed in this work are model compounds for the ease of demonstrating the functionality of the complexes; however, a next step would be to translate the understanding for use with commercial functional ingredients.

A key advantage of colloidal suspensions produced in this work is that they can be produced via currently used processing technologies, making them useful to have in the formulation tool-box. An additional processing step might be to include a drying step to yield a powdered product, which may be preferable for some commercial applications.

A next step would be to evaluate these structures for translation into food, pharmaceutical, and agrochemical products, both in terms of how they influence active/nutrient delivery (e.g. bioavailability and/or bioactivity) but also with respect to their bulk

material properties (e.g. rheology). The rheology of the coacervate suspensions would in particular be an interesting consideration since the complex suspensions (mixed biopolymer systems) appear qualitatively to have similar rheological properties to typical oil-in-water emulsions.

As chitosan is muco-adhesive it would also be beneficial to evaluate how this property is influenced by the presence of the protein, as well as how this could potentially influence active/nutrient bio-availability, bio-activity, and bio-efficacy in food, pharmaceutical, and agrochemical molecular delivery.

Acknowledgements

The authors acknowledge the Technology Strategy Board (TSB) and Engineering and Physical Research Council (EPSRC) in the UK for provision of funding to complete the research. Authors would also like to thank Phil Taylor and Pat Mulqueen at Syngenta Crop Protection for useful discussions.

References

- Anal, A. K., Tobiassen, A., Flanagan, J., & Singh, H. (2008). Preparation and characterization of nanoparticles formed by chitosan–caseinate interactions. *Colloids and Surfaces B: Biointerfaces*, 64, 104–110.
- Ausar, S. F., Bianco, I. D., Badini, R. G., Castagna, L. F., Modesti, N. M., Landa, C. A., et al. (2001). Characterization of casein micelle precipitation by chitosans. *Journal of Dairy Science*, 84, 361–369.
- Baldrick, P. (2010). The safety of chitosan as pharmaceutical excipient. *Regulatory Toxicology and Pharmacology*, 56, 290–299.
- Bugamelli, F., Raggi, M. A., Orienti, I., & Zecchi, V. (1998). Controlled insulin release from chitosan microparticles. *Archiv Der Pharmazie*, 331, 133–138.
- Chen, L., Remondetto, G. E., & Subirade, M. (2006). Food protein-based materials as nutraceutical delivery systems. *Trends in Food Science & Technology*, 17, 272–283.
- Dickinson, E. (1998). Stability and rheological implications of electrostatic milk protein-polysaccharide interactions. *Trends in Food Science & Technology*, 9, 347–354.
- Dickinson, E. (2006). Colloid science of mixed ingredients. *Soft Matter*, 2, 642–652.
- Dickinson, E. (2009). Hydrocolloids as emulsifiers and emulsion stabilizers. *Food Hydrocolloids*, 23, 1473–1482.
- Dickinson, E. (2012). Use of nanoparticles and microparticles in the formation and stabilization of food emulsions. *Trends in Food Science & Technology*, 24, 4–12.
- Doi, S., Clark, J. H., Macquarrie, D. J., & Milkowski, K. (2002). New materials based on renewable resources: chemically modified expanded corn starches as catalysts for liquid phase organic reactions. *Chemical Communications*, 22, 2632–2633.
- Girard, M., & Schaffer-Lequart, C. (2008). Attractive interactions between selected anionic exopolysaccharides and milk proteins. *Food Hydrocolloids*, 22, 1425–1434.
- Hack, B., Egger, H., Uhlemann, J., Henriet, M., Wirth, W., Vermeer, A. W. P., et al. (2012). Advanced agrochemical formulations through encapsulation strategies? *Chemie Ingenieur Technik*, 84, 223–234.
- Harnsilawat, T., Pongsawatmanit, R., & McClements, D. J. (2006). Characterization of β -lactoglobulin–sodium alginate interactions in aqueous solutions: a calorimetry, light scattering, electrophoretic mobility and solubility study. *Food Hydrocolloids*, 20, 577–585.
- Heurtault, B., Saulnier, P., Pech, B., Proust, J.-E., & Benoit, J.-P. (2003). Physico-chemical stability of colloidal lipid particles. *Biomaterials*, 24, 4283–4300.
- Hong, Y.-H., & McClements, D. J. (2007). Formation of hydrogel particles by thermal treatment of β -lactoglobulin–Chitosan complexes. *Journal of Agricultural & Food Chemistry*, 55, 5653–5660.
- Hosseini, S. M. H., Emam-Djomeha, Z., Razavia, S. H., Moosavi-Movahedib, A. A., Saboury, A. A., Mohammadifar, M. A., et al. (2013). Complex coacervation of β -lactoglobulin – κ -Carrageenan aqueous mixtures as affected by polysaccharide sonication. *Food Chemistry*, 141, 215–222.
- Huang, G.-Q., Sun, Y.-T., Xiao, J.-X., & Yang, J. (2012). Complex coacervation of soybean protein isolate and chitosan. *Food Chemistry*, 135, 534–539.
- Ikeda, S., & Nishinari, K. (2001). On solid-like rheological behaviors of globular protein solutions. *Food Hydrocolloids*, 15, 401–406.
- Kontogiorgos, V., Ritzoulis, C., Biliaderis, C. G., & Kasapis, S. (2006). Effect of barley β -glucan concentration on the microstructural and mechanical behaviour of acid-set sodium caseinate gels. *Food Hydrocolloids*, 20, 749–756.
- Lee, A.-C., & Hong, Y.-H. (2009). Coacervate formation of α -lactalbumin–chitosan and β -lactoglobulin–chitosan complexes. *Food Research International*, 42, 733–738.
- Macquarrie, D. J., & Hardy, J. J. E. (2005). Applications of functionalized chitosan in catalysis. *Industrial & Engineering Chemical Research*, 44, 8499–8520.

- Madene, A., Jacquot, M., Scher, J., & Desobry, S. (2006). Flavour encapsulation and controlled release – a review. *International Journal of Food Science & Technology*, 41, 1–21.
- Ogawa, S., Decker, E. A., & McClements, D. J. (2003). Production and characterization of O/W emulsions containing cationic droplets stabilized by lecithin-chitosan membranes. *Journal of Agricultural & Food Chemistry*, 51, 2806–2812.
- Ogawa, S., Decker, E. A., & McClements, D. J. (2004). Production and characterization of O/W emulsions containing droplets stabilized by lecithin-chitosan-pectin multilayered membranes. *Journal of Agricultural & Food Chemistry*, 52, 3595–3600.
- O'Sullivan, J., Arellano, M., Pichot, R., & Norton, I. T. (2014). The effect of ultrasound treatment on the structural, physical and emulsifying properties of dairy proteins. *Food Hydrocolloids*, 46, 386–396.
- Qin, Y. M., Zhu, C. J., Chen, J., & Zhong, J. H. (2007). Preparation and characterization of silver containing chitosan fibers. *Journal of Applied Polymer Science*, 104, 3622–3627.
- Rodríguez Patino, J. M., & Pilosof, A. M. R. (2011). Protein–polysaccharide interactions at fluid interfaces. *Food Hydrocolloids*, 25, 1925–1937.
- Semo, E., Kesselman, E., Danino, D., & Livney, Y. D. (2007). Casein micelle as a natural nano-capsular vehicle for nutraceuticals. *Food Hydrocolloids*, 21, 936–942.
- Sogias, I. A., Williams, A. C., & Khutoryanskiy, V. V. (2008). Why is chitosan mucoadhesive? *Biomacromolecules*, 9, 1837–1842.
- Sogias, I. A., Williams, A. C., & Khutoryanskiy, V. V. (2012). Chitosan-based mucoadhesive tablets for oral delivery of ibuprofen. *International Journal of Pharmaceutics*, 436, 602–610.
- Syrbe, A., Bauer, W. J., & Klostermeyer, N. (1998). Polymer science concepts in dairy systems – an overview of milk protein and food hydrocolloid interaction. *International Dairy Journal*, 8, 179–193.
- Tolstoguzov, V. B. (1991). Functional properties of food proteins and role of protein-polysaccharide interaction. *Food Hydrocolloids*, 4, 429–468.
- Tolstoguzov, V. (2003). Some thermodynamic considerations in food formulation. *Food Hydrocolloids*, 17, 1–23.
- Weinbreck, F., de Vries, R., Schrooyen, P., & de Kruif, C. G. (2003). Complex coacervation of whey proteins and gum Arabic. *Biomacromolecules*, 4, 293–303.
- Wu, T., Zivanovic, S., Hayes, D. G., & Weiss, J. (2008). Efficient reduction of chitosan molecular weight by high-intensity ultrasound: underlying mechanism and effect of process parameters. *Journal of Agricultural & Food Chemistry*, 56, 5112–5119.
- Yu, S., Hu, J., Pan, X., Yao, P., & Jiang, M. (2006). Stable and pH-sensitive nanogels prepared by self-assembly of chitosan and ovalbumin. *Langmuir*, 22, 2754–2759.